

Taming the growth

So far, this book has been concerned with the behaviour of QCD in the leading logarithmic approximation, which should be appropriate for large enough centre-of-mass energies and for those processes which satisfy the criteria relevant for the use of perturbative QCD. In Chapters 2–4, we derived and solved the BFKL equation. We were led to think of the Pomeron as the t -channel exchange of a pair of (interacting) reggeized gluons. In this chapter, we start off by reformulating the results already obtained for the elastic-scattering amplitude of two colourless states[†] in a way which suggests that we view the scattering as the incoherent scattering of individual colour dipoles whose locations in configuration space are frozen over the time of interaction. This approach will lead us to a very tangible physical picture of high energy scattering in configuration space.

In Section 8.2 we turn our attention to the undesirable feature which afflicts the scattering amplitudes calculated in the leading logarithm approximation. This is the violation of unitarity which results from the strong growth of the total cross-section with increasing energy. The dipole formalism discussed in Section 8.1 provides a very elegant framework in which to investigate the dominant corrections to the leading logarithm approximation which ensure that the theory remains unitary. We begin Section 8.2 by setting up an operator formalism (due to Mueller (1995)) to describe the dipole evolution and interaction. This formalism is subsequently used to incorporate the corrections which arise due to multiple dipole scattering effects (or, equivalently, the exchange of more than one Pomeron between the colliding hadrons) and ensure the unitarity of the scattering amplitude.

[†] We actually consider scattering of states whose leading Fock component is a heavy quark–antiquark pair, although our investigation is in principle much more general.

8.1 Dipole scattering

Let us start by defining, analogously to Eq.(4.46), the universal BFKL amplitude in impact parameter space, i.e.

$$\begin{aligned} \hat{f}(y, \mathbf{b}_1, \mathbf{b}'_1, \mathbf{b}_2, \mathbf{b}'_2) &= \frac{1}{(2\pi)^4} \partial_{\mathbf{b}_1}^2 \partial_{\mathbf{b}'_1}^2 \int d^2\mathbf{k}_1 d^2\mathbf{k}_2 d^2\mathbf{q} \\ &\times e^{i(\mathbf{k}_1 \cdot \mathbf{b}_{11'} - \mathbf{k}_2 \cdot \mathbf{b}_{22'} + \mathbf{q} \cdot (\mathbf{b}'_1 - \mathbf{b}'_2))} \frac{F(s, \mathbf{k}_1, \mathbf{k}_2, \mathbf{q})}{\mathbf{k}_2^2 (\mathbf{k}_1 - \mathbf{q})^2} \\ &= \frac{1}{(2\pi)^4} \int d^2\mathbf{k}_1 d^2\mathbf{k}_2 d^2\mathbf{q} \\ &\times e^{i(\mathbf{k}_1 \cdot \mathbf{b}_{11'} - \mathbf{k}_2 \cdot \mathbf{b}_{22'} + \mathbf{q} \cdot (\mathbf{b}'_1 - \mathbf{b}'_2))} \frac{\mathbf{k}_1^2}{\mathbf{k}_2^2} F(s, \mathbf{k}_1, \mathbf{k}_2, \mathbf{q}), \end{aligned} \tag{8.1}$$

where $F(s, \mathbf{k}_1, \mathbf{k}_2, \mathbf{q})$ is the usual BFKL amplitude which determines the scattering of two gluons, of transverse momenta \mathbf{k}_1 and \mathbf{k}_2 respectively, at energy s and with momentum transfer \mathbf{q} . It is obtained from $f(\omega, \mathbf{k}_1, \mathbf{k}_2, \mathbf{q})$ after inverting the ω -plane Mellin transform to reveal explicitly the energy, s , dependence. We use the notation where $y \equiv \ln(s/\mathbf{k}^2)$ and $\mathbf{b}_{11'} \equiv \mathbf{b}_1 - \mathbf{b}'_1$ (and similarly for $\mathbf{b}_{22'}$).

Using Eq.(4.52) and keeping only the $n = 0$ term in the sum over n we can write

$$\begin{aligned} \hat{f}(y, \mathbf{b}_1, \mathbf{b}'_1, \mathbf{b}_2, \mathbf{b}'_2) &= \frac{1}{(2\pi)^4} \int_{-\infty}^{\infty} d\nu \int d^2\mathbf{c} \frac{\nu^2}{(\nu^2 + 1/4)^2} e^{\bar{\alpha}_s \chi_0(\nu)y} \\ &\times \partial_{\mathbf{b}_1}^2 \partial_{\mathbf{b}'_1}^2 \tilde{\phi}_0^\nu(\mathbf{b}_1, \mathbf{b}'_1, \mathbf{c}) \tilde{\phi}_0^{\nu*}(\mathbf{b}_2, \mathbf{b}'_2, \mathbf{c}). \end{aligned} \tag{8.2}$$

Equation (4.51) then allows us to write

$$\begin{aligned} \hat{f}(y, \mathbf{b}_1, \mathbf{b}'_1, \mathbf{b}_2, \mathbf{b}'_2) &= \frac{1}{\pi^4} \int_{-\infty}^{\infty} d\nu \int d^2\mathbf{c} \frac{\nu^2}{\mathbf{b}_{11'}^4} e^{\bar{\alpha}_s \chi_0(\nu)y} \\ &\times \tilde{\phi}_0^\nu(\mathbf{b}_1, \mathbf{b}'_1, \mathbf{c}) \tilde{\phi}_0^{\nu*}(\mathbf{b}_2, \mathbf{b}'_2, \mathbf{c}). \end{aligned} \tag{8.3}$$

Now let us consider the convolution

$$\int d^2\mathbf{b}_x d^2\mathbf{b}'_x \hat{f}(y - y', \mathbf{b}_1, \mathbf{b}'_1, \mathbf{b}_x, \mathbf{b}'_x) \hat{f}(y', \mathbf{b}_x, \mathbf{b}'_x, \mathbf{b}_2, \mathbf{b}'_2).$$

Using the results (which we quote without proof and for details we refer to Lipatov (1986))

$$\int \frac{d^2\mathbf{b}_x d^2\mathbf{b}'_x}{\mathbf{b}_{xx'}^4} \tilde{\phi}_0^\nu(\mathbf{b}_x, \mathbf{b}'_x, \mathbf{c}) \tilde{\phi}_0^{\mu*}(\mathbf{b}_x, \mathbf{b}'_x, \mathbf{c}') \\ = \frac{\pi^4}{2\nu^2} \delta(\nu - \mu) \delta^2(\mathbf{c} - \mathbf{c}') + \frac{2^{4i\nu} i \pi^3}{\nu} \frac{\delta(\nu + \mu)}{|\mathbf{c} - \mathbf{c}'|^{2+4i\nu}}, \tag{8.4}$$

and

$$\int d^2\mathbf{c} \frac{\tilde{\phi}_0^{\nu*}(\mathbf{b}_1, \mathbf{b}'_1, \mathbf{c})}{|\mathbf{c} - \mathbf{c}'|^{2+4i\nu}} = \frac{\pi}{2i\nu} 2^{-4i\nu} \tilde{\phi}_0^\nu(\mathbf{b}_1, \mathbf{b}'_1, \mathbf{c}'), \tag{8.5}$$

one can derive the important result

$$\int d^2\mathbf{b}_x d^2\mathbf{b}'_x \hat{f}(y - y', \mathbf{b}_1, \mathbf{b}'_1, \mathbf{b}_x, \mathbf{b}'_x) \hat{f}(y', \mathbf{b}_x, \mathbf{b}'_x, \mathbf{b}_2, \mathbf{b}'_2) \\ = \hat{f}(y, \mathbf{b}_1, \mathbf{b}'_1, \mathbf{b}_2, \mathbf{b}'_2). \tag{8.6}$$

This is analogous to the $t = 0$ convolution of Eq.(5.2) and, as in that case, is true for arbitrary y' .

We can use Eq.(8.6) to factorize the BFKL amplitude in such a way that it can be absorbed into the definitions of the external impact factors. In particular, we can show (the details are included in Appendix A to this chapter) that

$$\frac{F(s, \mathbf{k}_1, \mathbf{k}_2, \mathbf{q})}{\mathbf{k}_2^2(\mathbf{k}_1 - \mathbf{q})^2} = \frac{1}{(2\pi)^6} \int d^2\mathbf{b}_{11'} d^2\mathbf{b}_{22'} \frac{d^2\mathbf{b}_{xx'}}{\mathbf{b}_{xx'}^2} \frac{d^2\mathbf{b}_{yy'}}{\mathbf{b}_{yy'}^2} \\ \times \frac{1}{4} \int \frac{d^2\mathbf{l}}{\mathbf{l}^2(1 - q)^2} N(b_{11'}, b_{xx'}, y', q) N(b_{22'}, b_{yy'}, y - y', q) \\ \times e^{-i(\mathbf{k}_1 - \mathbf{q}/2) \cdot \mathbf{b}_{11'}} e^{-i(\mathbf{k}_2 - \mathbf{q}/2) \cdot \mathbf{b}_{22'}} \\ \times \left[e^{i(\mathbf{q}-1) \cdot \mathbf{b}_{xx'}/2} - e^{-i(\mathbf{q}-1) \cdot \mathbf{b}_{xx'}/2} \right] \left[e^{i(\mathbf{q}-1) \cdot \mathbf{b}_{yy'}/2} - e^{-i(\mathbf{q}-1) \cdot \mathbf{b}_{yy'}/2} \right] \\ \times \left[e^{i\mathbf{l} \cdot \mathbf{b}_{xx'}/2} - e^{-i\mathbf{l} \cdot \mathbf{b}_{xx'}/2} \right] \left[e^{i\mathbf{l} \cdot \mathbf{b}_{yy'}/2} - e^{-i\mathbf{l} \cdot \mathbf{b}_{yy'}/2} \right]. \tag{8.7}$$

Again, non-boldface is used to denote the modulus of a two-vector. The **dipole number density** is defined by

$$N(r_0, r, y, q) \equiv \int_{-\infty}^{\infty} \frac{d\nu}{2\pi} V_q^{\nu*}(r_0) V_q^\nu(r) e^{\tilde{\alpha}_s \chi_0(\nu) y} \frac{r_0}{r}, \tag{8.8}$$

where

$$V_q^\nu(r) \equiv \frac{2i\nu}{\pi r} \int d^2\mathbf{R} e^{i\mathbf{q} \cdot \mathbf{R}} \left[\frac{\mathbf{r}^2}{(\mathbf{R} + \mathbf{r}/2)^2 (\mathbf{R} - \mathbf{r}/2)^2} \right]^{1/2+i\nu}. \tag{8.9}$$

It will soon become clear why we referred to $N(r_0, r, y, q)$ as the dipole number density, for now we take Eq.(8.8) as a definition of N .

To compute physical scattering amplitudes we need to perform the convolution with the appropriate impact factors, e.g. as in Eq.(4.36). For simplicity let us suppose that the external particles each contain only a single quark–antiquark pair, e.g. as would be the case for elastic photon–photon scattering.

In Chapter 7, we showed that the photon impact factor for $t = 0$ can be written in terms of the (light-cone) wavefunction of the photon, e.g. see Eqs.(7.25) and (7.27). In particular we derived the relation

$$\Phi(\mathbf{k}) = \frac{16\pi^2\alpha_s}{3} \int_0^1 dz \int d^2\mathbf{r} |\Psi(z, r)|^2 (1 - e^{i\mathbf{k}\cdot\mathbf{r}}). \quad (8.10)$$

The wavefunction, $\Psi(z, r)$, specifies the probability that the photon has fluctuated into the $q\bar{q}$ pair of transverse size r and with their momentum partitioned in the ratio $z : (1 - z)$.

Equation (8.10) is quite general. By this we mean that for any impact factor, which describes the interaction of a $q\bar{q}$ pair with the two gluons of the Pomeron, we can always write down the corresponding wavefunction and factorize off the factor $(1 - e^{i\mathbf{k}\cdot\mathbf{r}})$. We shall subsequently refer to the generic $q\bar{q}$ system as an **onium** state. Let us recall the origin of the $(1 - e^{i\mathbf{k}\cdot\mathbf{r}})$ factor in Eq.(8.10). From Eqs.(7.23), (7.24) and (7.25) we see that the factor of unity arises from those two graphs where the gluons couple to the same quark (or antiquark) in the onium. The second, exponential, factor derives from the coupling to both the quark and antiquark of the onium. The cancellation between these two types of graph, which occurs whenever one of the two gluons goes on shell (and hence ensures the finiteness of the scattering amplitude), has been explicitly displayed in this factor. The above discussion was specific to the case of zero momentum transfer (i.e. $\mathbf{q} = \mathbf{0}$). For non-zero momentum transfer we have the following general relation between the impact factor and the onium wavefunction:

$$\begin{aligned} \Phi(\mathbf{k}) &= \frac{8\pi^2\alpha_s}{3} \int_0^1 dz \int d^2\mathbf{r} |\Psi(z, r)|^2 \\ &\times (e^{i\mathbf{k}\cdot\mathbf{r}/2} - e^{-i\mathbf{k}\cdot\mathbf{r}/2})(e^{i(\mathbf{q}-\mathbf{k})\cdot\mathbf{r}/2} - e^{-i(\mathbf{q}-\mathbf{k})\cdot\mathbf{r}/2}). \end{aligned} \quad (8.11)$$

To re-iterate, by working in the co-ordinate space representation

the formation of the onium state is determined by the wavefunction factor $|\Psi(z, r)|^2$ and this can be cleanly factorized from the coupling of the $q-\bar{q}$ pair to the Pomeron (contained in the exponential factors). This is consistent with the space-time picture presented in the preceding chapter (see Section 7.3). We say that the dependence on the onium wavefunction factorizes from the coupling of the dipole ($q-\bar{q}$ pair of fixed size \mathbf{r}) to the two gluons of the Pomeron.

The elastic-scattering amplitude of two onium states, with wavefunctions $\Psi_1(z_1, r_1)$ and $\Psi_2(z_2, r_1)$, respectively, can now be written:

$$\begin{aligned} \frac{\Im m A(s, t)}{s} &= \frac{8}{9} \int dz_1 dz_2 \int d^2\mathbf{r}_1 d^2\mathbf{r}_2 |\Psi_1(z_1, r_1)|^2 |\Psi_2(z_2, r_2)|^2 \\ &\times \alpha_s^2 \int \frac{d^2\mathbf{b}_{\mathbf{x}\mathbf{x}'}}{2\pi\mathbf{b}_{\mathbf{x}\mathbf{x}'}} \frac{d^2\mathbf{b}_{\mathbf{y}\mathbf{y}'}}{2\pi\mathbf{b}_{\mathbf{y}\mathbf{y}'}} \int \frac{d^2\mathbf{l}}{\mathbf{l}^2(1-\mathbf{q})^2} \\ &\times N(r_1, \mathbf{b}_{\mathbf{x}\mathbf{x}'}, \mathbf{y}', q) N(r_2, \mathbf{b}_{\mathbf{y}\mathbf{y}'}, \mathbf{y} - \mathbf{y}', q) \\ &\times \left[e^{i(\mathbf{q}-1)\cdot\mathbf{b}_{\mathbf{x}\mathbf{x}'}/2} - e^{-i(\mathbf{q}-1)\cdot\mathbf{b}_{\mathbf{x}\mathbf{x}'}/2} \right] \left[e^{i(\mathbf{q}-1)\cdot\mathbf{b}_{\mathbf{y}\mathbf{y}'}/2} - e^{-i(\mathbf{q}-1)\cdot\mathbf{b}_{\mathbf{y}\mathbf{y}'}/2} \right] \\ &\times \left[e^{i\mathbf{l}\cdot\mathbf{b}_{\mathbf{x}\mathbf{x}'}/2} - e^{-i\mathbf{l}\cdot\mathbf{b}_{\mathbf{x}\mathbf{x}'}/2} \right] \left[e^{i\mathbf{l}\cdot\mathbf{b}_{\mathbf{y}\mathbf{y}'}/2} - e^{-i\mathbf{l}\cdot\mathbf{b}_{\mathbf{y}\mathbf{y}'}/2} \right]. \end{aligned} \tag{8.12}$$

This is obtained from Eqs.(4.36) and (8.7) by substituting the defining relation Eq.(8.11) for each impact factor and integrating over \mathbf{k}_1 and \mathbf{k}_2 (these integrals just yield delta functions which fix the size of the parent dipole plus terms which vanish since $N(0, r, y, q) = 0$). The colour factor $\mathcal{G} = N^2 G_0^{(1)} = 2$.

Equation (8.12) has a very appealing physical interpretation. To see this let us first consider the amplitude in the approximation that the onia interact through the exchange of two gluons. In this case we have

$$\begin{aligned} \frac{\Im m A(s, t)}{s} &= \frac{2}{(2\pi)^4} \int \frac{d^2\mathbf{l}}{\mathbf{l}^2(1-\mathbf{q})^2} \Phi_1(\mathbf{l}, \mathbf{q}) \Phi_2(\mathbf{l}, \mathbf{q}) \\ &= \frac{8}{9} \alpha_s^2 \int dz_1 dz_2 \int d^2\mathbf{r}_1 d^2\mathbf{r}_2 |\Psi_1(z_1, r_1)|^2 |\Psi_2(z_2, r_2)|^2 \\ &\int \frac{d^2\mathbf{l}}{\mathbf{l}^2(1-\mathbf{q})^2} \left[e^{i\mathbf{l}\cdot\mathbf{r}_1/2} - e^{-i\mathbf{l}\cdot\mathbf{r}_1/2} \right] \left[e^{i(\mathbf{q}-1)\cdot\mathbf{r}_1/2} - e^{-i(\mathbf{q}-1)\cdot\mathbf{r}_1/2} \right] \\ &\left[e^{i\mathbf{l}\cdot\mathbf{r}_2/2} - e^{-i\mathbf{l}\cdot\mathbf{r}_2/2} \right] \left[e^{i(\mathbf{q}-1)\cdot\mathbf{r}_2/2} - e^{-i(\mathbf{q}-1)\cdot\mathbf{r}_2/2} \right]. \end{aligned} \tag{8.13}$$

This equation is shown graphically in Fig. 8.1, where the factoriza-

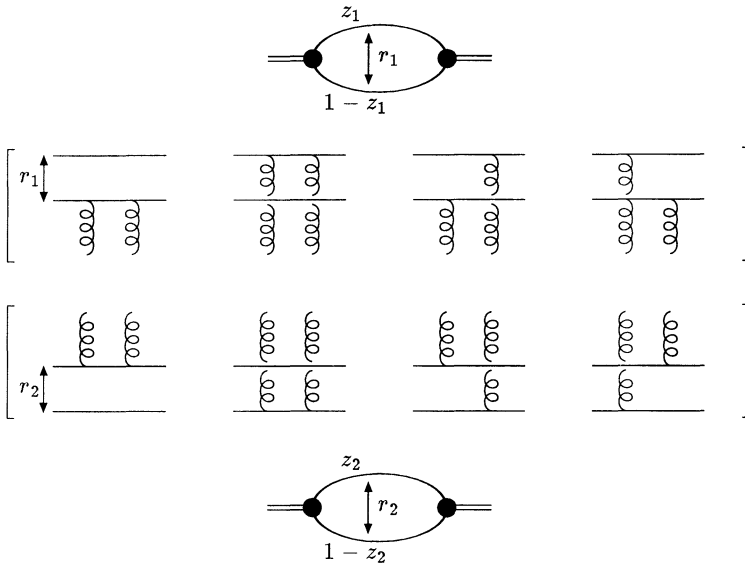


Fig. 8.1. Diagrammatic illustration of the dipole factorization explicit in Eq.(8.13).

tion of the onia wavefunctions from the dipole–dipole interaction cross-section is illustrated.

Comparing Eq.(8.13) with Eq.(8.12) we see some striking similarities. The only new factors are those associated with what we have termed the dipole number densities, N . In particular, the exponential factors are equivalent. This similarity means that we can interpret the elastic scattering of the two onia in terms of the scattering of individual dipoles in each onium state off those in the other state (since the dipole–dipole interaction cross-section is explicit in Eq.(8.12)). The number density of dipoles is then indeed given by the function $N(b, r, y, q)$. It specifies the number density of dipoles of size r inside an onium whose primary dipole (i.e. the $q\bar{q}$ pair) has size b and which lie within y units of rapidity of the parent onium. The q -dependence is present since the number density depends upon the angle through which the onia scatter. Equivalently, we could take the Fourier transform with respect to q and obtain the number densities as a function of their displace-

ment from the parent onia (indeed, we shall do this at the end of this section). The normalization has been chosen such that

$$\int \frac{d^2\mathbf{r}}{2\pi r^2} N(b, r, y, q)$$

is the total number of dipoles inside the parent dipole.

Note that the dipole number density at $q = 0$ and large enough y is the familiar looking expression (e.g. see Eq.(4.34)):

$$N(b, r, y, 0) \approx \frac{b}{r} \frac{e^{\omega_0 y}}{(\pi a^2 y)^{1/2}} \exp\left(-\frac{\ln^2(b^2/r^2)}{4a^2 y}\right). \quad (8.14)$$

In addition, we note that it is not meaningful to associate in a unique way the dipoles with the colliding onia. By picking $y' = 0$, $N(r_1, b_{xx'}, 0, q) = r_1 \delta(r_1 - b_{xx'})$ and all the dipoles are identified as being radiated from the parent dipole of size r_2 (i.e. from the onium which has wavefunction Ψ_2). By picking $y' = y/2$ we have the democratic scenario where the dipoles are ‘shared’ between the colliding onia.

So, we have been forced into the interpretation of onium–onium scattering in terms of the interaction between ‘child’ dipoles (the parents being the $q-\bar{q}$ pairs of the onia); the interaction being none other than the two-gluon exchange between the two child dipoles. It is natural to ask how these dipoles originate. We know from the above that we have succeeded in factorizing the BFKL physics associated with the ladder of reggeized gluons into the dipole density functions. What has happened? Let us think in a frame where the two onia are colliding in their centre of mass. We can then identify a left-moving onium and a right-moving onium. Now consider the left-moving onium. The parent dipole is created a long time before the interaction with a dipole in the other onium. This parent dipole can then radiate a soft gluon. In terms of its colour structure the emitted gluon can be viewed as a $3 \otimes \bar{3}$ state (i.e. like a quark–antiquark pair). This view of the gluon is appropriate in the formal limit where the number of colours, N , is large. This means that the leading logarithm approximation is also the leading N approximation – indeed we can see this by noting that the relevant coupling for soft gluon emission is $\bar{\alpha}_s$, (i.e. the strong coupling is always accompanied by a factor of N). The quark line from this gluon and the antiquark line of the parent dipole then form a secondary dipole, and similarly for the quark line of the

gluon and the antiquark line of the parent. *So the emission of a gluon corresponds to the annihilation of the parent dipole and the creation of two new secondary dipoles.* This branching continues until there is no more rapidity for further emission and so the parent left-moving onium can be viewed as a collection of colour dipoles. The same can be said about the right-moving onium: it, too, is an assembly of dipoles. The onia then interact with each other through the scattering of their constituent dipoles which, in the one Pomeron exchange approximation (which is the BFKL approximation), scatter via exchange of two gluons. The left and right-moving dipoles then re-assemble to generate the final state onia. In this way we are able to understand the origin of the dipole factorization which is explicit in Eq.(8.12).

Before leaving this section, let us first re-cast Eq.(8.12) so that it explicitly exhibits the dependence of the scattering amplitude on the impact parameter of the collision (i.e. we take a Fourier transform to eliminate the \mathbf{q} -dependence).

Defining the scattering amplitude for collisions between two onia at impact parameter \mathbf{b} via

$$A(b, y) = \int \frac{d^2\mathbf{q}}{(2\pi)^2} e^{-i\mathbf{q}\cdot\mathbf{b}} \frac{A(s, t)}{2s} \quad (8.15)$$

allows us to write

$$A(b, y) = -i \frac{8}{9} \int dz_1 dz_2 \int d^2\mathbf{r}_1 d^2\mathbf{r}_2 |\Psi_1(z_1, r_1)|^2 |\Psi_2(z_2, r_2)|^2 \times F(r_1, r_2, b, y), \quad (8.16)$$

where $F(r_1, r_2, b, y)$ is the amplitude for the elastic scattering of a pair of dipoles of respective sizes r_1 and r_2 at an impact parameter b . Explicitly it is given by

$$F(r_1, r_2, b, y) = - \int \frac{d^2\mathbf{b}_{\mathbf{x}\mathbf{x}'}}{2\pi\mathbf{b}_{\mathbf{x}\mathbf{x}'}} \int \frac{d^2\mathbf{b}_{\mathbf{y}\mathbf{y}'}}{2\pi\mathbf{b}_{\mathbf{y}\mathbf{y}'}} \int d^2\mathbf{R} d^2\mathbf{R}' \times n(r_1, b_{\mathbf{x}\mathbf{x}'}, y', R) n(r_2, b_{\mathbf{y}\mathbf{y}'}, y - y', |\mathbf{R}' - \mathbf{b}|) \times f(\mathbf{R} - \mathbf{R}', \mathbf{b}_{\mathbf{x}\mathbf{x}'}, \mathbf{b}_{\mathbf{y}\mathbf{y}'}), \quad (8.17)$$

where

$$\begin{aligned}
 f(\mathbf{R}, \mathbf{b}, \mathbf{c}) &= \frac{\alpha_s^2}{2} \int \frac{d^2\mathbf{q}}{(2\pi)^2} e^{-i\mathbf{q}\cdot\mathbf{R}} \int \frac{d^2\mathbf{l}}{\mathbf{l}^2(1-\mathbf{q})^2} \\
 &\times \left[e^{i(\mathbf{q}-1)\cdot\mathbf{b}/2} - e^{-i(\mathbf{q}-1)\cdot\mathbf{b}/2} \right] \left[e^{i(\mathbf{q}-1)\cdot\mathbf{c}/2} - e^{-i(\mathbf{q}-1)\cdot\mathbf{c}/2} \right] \\
 &\times \left[e^{i\mathbf{l}\cdot\mathbf{b}/2} - e^{-i\mathbf{l}\cdot\mathbf{b}/2} \right] \left[e^{i\mathbf{l}\cdot\mathbf{c}/2} - e^{-i\mathbf{l}\cdot\mathbf{c}/2} \right]. \tag{8.18}
 \end{aligned}$$

The number density of dipoles, of size \mathbf{x} within a parent dipole of size \mathbf{x}_0 within the rapidity y and at a distance \mathbf{r} of the parent is $n(x_0, x, y, r)$, where

$$n(x_0, x, y, r) = \int \frac{d^2\mathbf{q}}{(2\pi)^2} e^{-i\mathbf{q}\cdot\mathbf{r}} N(x_0, x, y, q). \tag{8.19}$$

Representing the amplitude exclusively in terms of the positions and sizes of the dipoles will be convenient when we come to discuss the multiple scattering corrections in the next section. For now, let us express the optical theorem in terms of $A(b, y)$; it is simply

$$\sigma_{\text{tot}}(y) = 2\pi \int db^2 \Im mA(b, y). \tag{8.20}$$

Our normalization of the amplitude is such that $\Im mA(b, y) = \theta(b_0 - b)$ in the black disc limit (i.e. totally absorbtive scattering).

To close this section, we note that by taking Eqs.(8.8) and (8.9), expanding $\chi_0(\nu)$ up to quadratic order in ν and integrating over ν using the saddle point approximation we arrive at the approximation

$$\begin{aligned}
 n(x_0, x, y, r) &\approx \frac{2x_0}{xr^2} \ln \left(\frac{16r^2}{xx_0} \right) \frac{e^{\omega_0 y}}{(\pi a^2 y)^{3/2}} \\
 &\times \exp \left(-\frac{\ln^2(16r^2/xx_0)}{a^2 y} \right), \tag{8.21}
 \end{aligned}$$

provided $r \gg x, x_0$ and $a^2 y \gg \ln(r^2/xx_0)$. Compare this with the result of the preceding chapter, Eq.(7.14). The diffusion properties of the BFKL equation are manifest as diffusion in the dipole sizes with increasing rapidity. The displacement of the child dipole from the parent acts as an effective cut-off on the size of the largest dipoles that can be created.

8.2 Unitarity

One of the main results which is obtained in the leading logarithmic approximation used to derive the BFKL equation is that the elastic scattering amplitudes rise with increasing centre-of-mass energy, s , as some power of s . Through the optical theorem this then translates into a corresponding growth of the total cross-section, i.e.

$$\sigma_{\text{tot}} \sim s^{\omega_0}, \quad (8.22)$$

where $\omega_0 = 4\bar{\alpha}_s \ln 2$. We should ask whether this is sensible behaviour in the limit $s \rightarrow \infty$. Intuitively, if the strong interactions are of finite range then we expect the asymptotic behaviour of total cross-sections to be limited in some way. This physics is missing in the leading logarithmic approximation. Moreover, in Chapter 1 we quoted the Froissart–Martin bound, which states that total cross-sections cannot rise (in the limit $s \rightarrow \infty$) faster than $\ln^2 s$ (see Eq.(1.25)). Although this bound may well become significant only at energies well beyond those which are feasibly accessible it is important to understand how the leading logarithmic approximation is corrected to account for the unitarization corrections which eventually bring the theory into agreement with the Froissart–Martin bound. The study of unitarity corrections within perturbative QCD is the subject of the remainder of this chapter.

We start by providing a physical argument (originally due to Feynman) which makes the Froissart–Martin bound plausible. Let us suppose that the target particle has some density distribution which reflects the short range nature of the strong force, e.g.

$$\rho(r) = \rho_0 \exp(-r/R), \quad (8.23)$$

where r is the distance from the centre of the target and R characterizes the size of the target. It is important that this distribution falls off faster than any power at large distances (which we take as a fundamental property of the strong interactions). If the probability of an interaction between the beam particle with the target is bounded (as $s \rightarrow \infty$) by some finite power of s then the interaction probability satisfies

$$P(s, r) < P_0 \left(\frac{s}{s_0} \right)^N \exp(-r/R). \quad (8.24)$$

Hence, the interaction will be negligible for collisions at impact parameters

$$r > NR \ln(s/s_0)$$

and so the total cross-section satisfies

$$\sigma_{\text{tot}} < \pi R^2 N^2 \ln^2(s/s_0). \quad (8.25)$$

It is possible to derive the Froissart–Martin bound in a more rigorous fashion starting from the partial wave expansion and assuming the amplitude to satisfy (subtracted) dispersion relations (this is the assumption that the amplitude is bounded by a finite power in s). It arises as a direct consequence of the unitarity of the individual partial wave amplitudes and the existence of some lowest mass bound state whose mass is different from zero (i.e. the pion) (see e.g. Collins (1977), Martin, Morgan & Shaw (1976)). This latter property, which is equivalent to demanding that the strong force be short range, is one which we do not expect to be able to accommodate in our perturbative calculations, as such we might well be able to successfully unitarize the scattering amplitude but fail to satisfy the Froissart–Martin bound.

Clearly, therefore, all our previous calculations based on QCD in the leading logarithm approximation must break down as the centre-of-mass energy tends to infinity. In the centre-of-mass frame of the colliding particles the increase of the total cross-section with energy is due to the proliferation of soft gluon emissions. The power-like increase in the number of soft gluons means a corresponding rise in the total cross-section. In the dipole language it is the proliferation of dipoles which drives the rise. It is not hard to imagine the physics which must eventually enter as the spatial density of gluons (dipoles) continues to increase. Ultimately, the density will be large enough such that *more than one pair of dipoles will undergo a scattering* for each parent particle collision. There is also the possibility that a dipole in the parent can scatter off other dipoles also within the parent. As we shall see the distinction between these two forms of correction is frame dependent. Not surprisingly both forms of correction lead to a taming of the growth of the elastic scattering amplitude (and hence total cross-section) in line with the demands of unitarity. It is the purpose of the remainder of this chapter to describe the multiple scattering mechanism in more detail.

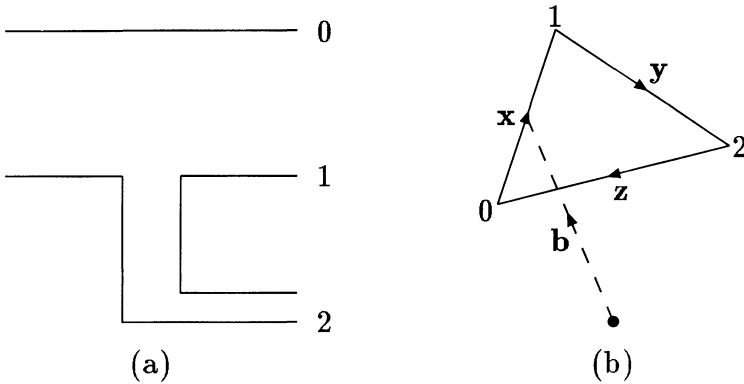


Fig. 8.2. (a) Fundamental dipole vertex used to generate the dipole evolution. A gluon is emitted at position 2. (b) The vectors which specify the size and position of the parent and child dipoles.

8.2.1 The operator formalism

We start by introducing an operator formalism (Mueller (1995)) which can be used to re-derive the BFKL equation but which will also be suitable for a quantitative study of the leading multiple scattering corrections. We have shown that high energy scattering between two onia can be viewed as a two-step process. Firstly, a cloud of dipoles is evolved around each of the primary dipoles. This dipole evolution can be described as a classical branching process in impact parameter space. Secondly, the dipole clouds interact with each other so that the total cross-section is an incoherent sum over the individual dipole-dipole cross-sections. The nature of the dipole branching process suggests that we should be able to describe it using an operator formalism where the basic operators are dipole creation and annihilation operators. There is a fundamental vertex which describes the branching of an initial dipole into two secondary dipoles and it is the successive iteration of this basic vertex that determines the evolution of the dipole cloud.

We begin by deriving an expression for the fundamental dipole vertex illustrated in Fig. 8.2(a). The parent dipole (specified by the points denoted 0 and 1) radiates a gluon at point 2 which generates

the child dipoles (of sizes y and z , see Fig. 8.2(b)). Firstly, we introduce dipole creation and annihilation operators $a^\dagger(\mathbf{b}, \mathbf{x})$ and $a(\mathbf{b}, \mathbf{x})$ respectively (\mathbf{b} is the location of the dipole centre and \mathbf{x} is its size). Since the dipoles satisfy bosonic statistics we impose the commutation relation

$$[a(\mathbf{b}, \mathbf{x}), a^\dagger(\mathbf{b}', \mathbf{x}')] = \delta^{(2)}(\mathbf{b} - \mathbf{b}')\delta^{(2)}(\mathbf{x} - \mathbf{x}'). \tag{8.26}$$

The differential probability for the emission of a gluon off a dipole of size \mathbf{r} into the rapidity interval $y \rightarrow y + dy$ and with transverse momentum $\mathbf{k} \rightarrow \mathbf{k} + d^2\mathbf{k}$ is

$$d^3P = \bar{\alpha}_s \frac{d^2\mathbf{k}}{\pi\mathbf{k}^2} dy (1 - e^{i\mathbf{k}\cdot\mathbf{r}}). \tag{8.27}$$

For the derivation of this expression we refer to Appendix B of this chapter. The colour factor is appropriate for purely gluonic branching, i.e. we need an adjustment which accounts for the different coupling to the primary dipole, which is a $q-\bar{q}$ pair. This is the origin of the colour factor of $\frac{8}{9}$ which sits outside the amplitude, e.g. Eq.(8.16).[†] This very simple form is, however, unsuitable for the dipole evolution. We need to obtain an expression in terms of the relevant dipole sizes. Starting from

$$\int \frac{d^2\mathbf{k}}{\mathbf{k}^2} e^{i\mathbf{k}\cdot\mathbf{r}} = \int d^2\mathbf{k} \frac{\mathbf{k}\cdot\mathbf{k}}{\mathbf{k}^4} e^{i\mathbf{k}\cdot\mathbf{r}} \tag{8.28}$$

and using

$$\frac{\mathbf{k}_i}{\mathbf{k}^2} = \frac{1}{2\pi i} \int \frac{d^2\mathbf{x}}{\mathbf{x}^2} \mathbf{x}_i e^{i\mathbf{k}\cdot\mathbf{x}} \tag{8.29}$$

yields

$$\int \frac{d^2\mathbf{k}}{\mathbf{k}^2} e^{i\mathbf{k}\cdot\mathbf{r}} = - \int d^2\mathbf{x}_1 d^2\mathbf{x}_2 \frac{\mathbf{x}_1 \cdot \mathbf{x}_2}{\mathbf{x}_1^2 \mathbf{x}_2^2} \delta^{(2)}(\mathbf{x}_1 + \mathbf{x}_2 + \mathbf{r}). \tag{8.30}$$

Thus we can write

$$\begin{aligned} \frac{d^3P}{dy} &= \frac{\bar{\alpha}_s}{2\pi} d^2\mathbf{x}_1 d^2\mathbf{x}_2 \delta^{(2)}(\mathbf{x}_1 + \mathbf{x}_2 + \mathbf{r}) \left(\frac{(\mathbf{x}_1 + \mathbf{x}_2)^2}{\mathbf{x}_1^2 \mathbf{x}_2^2} \right) \\ &= \frac{\bar{\alpha}_s}{2\pi} d^2\mathbf{x}_1 d^2\mathbf{x}_2 \delta^{(2)}(\mathbf{x}_1 + \mathbf{x}_2 + \mathbf{r}) \left(\frac{r^2}{x_1^2 x_2^2} \right). \end{aligned} \tag{8.31}$$

[†] This factor is equal to $1 - 1/N^2$ and as such is equal to unity in the leading N approximation where there is no difference between the colour structure of the gluon and that of a $q-\bar{q}$ pair.

This form is now suitable for use in the dipole evolution since it describes the branching of the parent dipole of size r into two new dipoles of sizes x_1 and x_2 . Each of these secondary dipoles can then act as a source for further gluon emission, the probability of which can be computed using Eq.(8.31), and so on.

In the operator language, the basic vertex for dipole creation is thus

$$V_1[a^\dagger, a] = \frac{\bar{\alpha}_s}{2\pi} \int d^2\mathbf{b} d^2\mathbf{x} d^2\mathbf{y} d^2\mathbf{z} \delta^{(2)}(\mathbf{x} + \mathbf{y} + \mathbf{z}) \\ \times \frac{x^2}{y^2 z^2} a^\dagger(\mathbf{b} + \mathbf{y}/2, \mathbf{z}) a^\dagger(\mathbf{b} - \mathbf{z}/2, \mathbf{y}) a(\mathbf{b}, \mathbf{x}). \quad (8.32)$$

The square brackets indicate that it is a functional of the creation and annihilation operators. The dipole evolution is driven by this vertex. The arguments of the dipole operators can be seen from Fig. 8.2(b). However, things are not quite so simple. Recall that the BFKL equation contains essential virtual corrections. These corrections are so far absent. However, we can construct the correction, V_2 , to the basic vertex, V_1 , which accounts for all the virtual graphs. The vertex V_1 possesses ultra-violet divergences whenever the emitted dipoles have vanishing size (i.e. $y \rightarrow 0$ or $z \rightarrow 0$). In order to regularize these divergences we introduce a lower cut-off ρ on the size of the emitted dipoles. The virtual graphs are accounted for through the vertex

$$V_2[a^\dagger, a] = -\frac{\bar{\alpha}_s}{2\pi} \int d^2\mathbf{b} d^2\mathbf{x} d^2\mathbf{y} d^2\mathbf{z} \delta^{(2)}(\mathbf{x} + \mathbf{y} + \mathbf{z}) \\ \times \frac{x^2}{y^2 z^2} a^\dagger(\mathbf{b}, \mathbf{x}) a(\mathbf{b}, \mathbf{x}) \\ \approx -\bar{\alpha}_s \int d^2\mathbf{b} d^2\mathbf{x} \ln \frac{x^2}{\rho^2} a^\dagger(\mathbf{b}, \mathbf{x}) a(\mathbf{b}, \mathbf{x}). \quad (8.33)$$

This form is determined by requiring the conservation of probability, i.e. the total probability to create a pair of secondary dipoles integrated over all the sizes of these dipoles, plus the probability *not* to create a secondary pair must be unity. We demonstrate this to order α_s below. The approximate equality on the second line of Eq.(8.33) is valid in the limit of small ρ . The complete vertex for dipole evolution is then

$$V[a^\dagger, a] = V_1[a^\dagger, a] + V_2[a^\dagger, a]$$

and is independent of ρ (as $\rho \rightarrow 0$).

We are now in a position to construct the S -matrix for the scattering of primary dipoles of sizes r_1 and r_2 (it will give us $F(r_1, r_2, b, y)$ of Eq.(8.17)). Consider the centre-of-mass scattering of the two primary dipoles (we refer to them as left-moving and right-moving). The left-moving dipole (at position \mathbf{b}_0 and of size \mathbf{r}_1) is the state

$$|\mathbf{b}_0, \mathbf{r}_1\rangle = a^\dagger(\mathbf{b}_0, \mathbf{r}_1)|0\rangle, \tag{8.34}$$

where $\langle 0|0\rangle = 1$. Similarly, the right-moving dipole (which is at impact parameter \mathbf{b} relative to the left mover) is the state

$$|\mathbf{b} + \mathbf{b}_0, \mathbf{r}_2\rangle = d^\dagger(\mathbf{b} + \mathbf{b}_0, \mathbf{r}_2)|0\rangle, \tag{8.35}$$

where d and d^\dagger are the annihilation and creation operators for the right movers (we need independent operators since the two dipole clouds evolve independently, i.e. the left mover operators commute with the right mover operators). The probability of finding the primary left mover dipole in a configuration of n dipoles with positions and sizes $\{\mathbf{b}_1, \mathbf{c}_1; \mathbf{b}_2, \mathbf{c}_2; \dots; \mathbf{b}_n, \mathbf{c}_n\}$ is thus

$$\frac{d^{4n} p_n}{d^2 \mathbf{b}_1 d^2 \mathbf{c}_1 \dots d^2 \mathbf{b}_n d^2 \mathbf{c}_n} = \langle 0|a(\mathbf{b}_1, \mathbf{c}_1) \dots a(\mathbf{b}_n, \mathbf{c}_n) e^{yV_L} a^\dagger(\mathbf{b}_0, \mathbf{r}_1)|0\rangle. \tag{8.36}$$

We have used the subscript L to denote that the vertex operator acts on left movers. The basic vertex appears in the exponential due to the combinatorial factorial factor which is needed on iterating the basic vertex (recall that the vertex integrates over all dipole configurations). A similar expression exists for the evolution of the right movers. It is convenient to define the n -dipole state (integrated over all dipole locations and sizes):

$$|n\rangle \equiv \frac{1}{n!} \int \left(\prod_{j=1}^n d^2 \mathbf{c}_j d^2 \mathbf{b}_j a^\dagger(\mathbf{b}_j, \mathbf{c}_j) \right) |0\rangle. \tag{8.37}$$

The integrated probability for the n -dipole configuration is then

$$\begin{aligned} P_n &= \frac{1}{n!} \int d^{4n} p_n \\ &= \langle n|e^{yV_L} a^\dagger(\mathbf{b}_0, \mathbf{r}_1)|0\rangle, \end{aligned} \tag{8.38}$$

and satisfies

$$\sum_{n=1}^{\infty} P_n = 1, \tag{8.39}$$

which is consistent with our interpretation of P_n as a probability. Working to first order in α_s allows us to see the conservation of probability and the role of the virtual corrections (V_2) explicitly. At this order, only P_1 and P_2 are non-zero and it is easy to show that

$$\begin{aligned} P_1 &= 1 - \bar{\alpha}_s \ln \frac{r_1^2}{\rho^2}, \\ P_2 &= \bar{\alpha}_s \ln \frac{r_1^2}{\rho^2}. \end{aligned} \tag{8.40}$$

The dependence upon the ultra-violet cut-off (ρ) cancels, as required. Moreover, the virtual corrections generated by V_2 are solely responsible for the logarithmic term in P_1 which ensures the conservation of probability.

The scattering matrix for the elastic scattering of the left- and right-moving primary dipoles is given by

$$S(\mathbf{r}_1, \mathbf{r}_2, \mathbf{b}, y) = \langle 0 | e^{a_1 + d_1} e^{-f} e^{y' V_L + (y - y') V_R} d^\dagger(\mathbf{b} + \mathbf{b}_0, \mathbf{r}_2) a^\dagger(\mathbf{b}_0, \mathbf{r}_1) | 0 \rangle, \tag{8.41}$$

where

$$a_1 = \int d^2 \mathbf{b} d^2 \mathbf{c} a(\mathbf{b}, \mathbf{c}) \tag{8.42}$$

(and similarly for d_1). The dipole-dipole scattering operator, f , is given by

$$\begin{aligned} f &= \int d^2 \mathbf{R} d^2 \mathbf{R}' d^2 \mathbf{c} d^2 \mathbf{c}' f(\mathbf{R} - \mathbf{R}', \mathbf{c}, \mathbf{c}') \\ &\quad \times d^\dagger(\mathbf{R}, \mathbf{c}) d(\mathbf{R}, \mathbf{c}) a^\dagger(\mathbf{R}', \mathbf{c}') a(\mathbf{R}', \mathbf{c}') \end{aligned} \tag{8.43}$$

and $f(\mathbf{R} - \mathbf{R}', \mathbf{c}, \mathbf{c}')$ is given in Eq.(8.18). A few words are in order regarding Eq.(8.41). Starting from the ‘vacuum state’ on the right, we first create the primary dipoles (of size \mathbf{r}_1 and \mathbf{r}_2 with relative separation \mathbf{b}). The action of the dipole evolution operators then generates the respective dipole clouds. These clouds are then made to interact. The amplitude for any single dipole-dipole interaction is given by $-f$ (the operator structure of Eq.(8.43) is such that it projects out the dipoles that interact from the

evolved dipole clouds). If we assume that there are very many dipoles and that these dipoles scatter independently of each other then we are able to account for an arbitrary number of individual dipole–dipole interactions by including the factor $(-f)^n/n!$ for n dipole–dipole interactions. This explains the origin of the factor e^{-f} in Eq.(8.41). The final factor simply ensures that the dipole systems have unit overlap with the final state. The factorial factors associated with the various exponential terms are necessary in order to divide out the equivalent configurations (recall that all secondary dipole configurations are integrated over to determine the elastic amplitude). Thus we have a formalism which allows us to include the **multiple scattering** of individual dipoles. As we shall soon see, the BFKL (leading logarithmic approximation) is equivalent to including only the interaction of a single pair of dipoles (which eventually violates unitarity) whilst the complete multiple scattering series ensures that unitarity is preserved.

We can re-write the S -matrix in an alternative form by inserting the unit operator,

$$\sum_{m,n} |n, m\rangle \langle n, m|, \quad (8.44)$$

where the state $|n, m\rangle = |n\rangle|m\rangle$ represents n dipoles in the left-moving onium and m dipoles in the right-moving onium. We find

$$S(\mathbf{r}_1, \mathbf{r}_2, \mathbf{b}, y) = \sum_{m,n} P_n P_m \exp(-\langle n, m|f|n, m\rangle). \quad (8.45)$$

Note that this expression explicitly satisfies the constraints of unitarity. To see this we note that $|1 - S|^2$ is the probability of an elastic scattering occurring at a fixed impact parameter and as such should satisfy $|1 - S|^2 \leq 1$. This bound is indeed satisfied since the P_n and P_m are probabilities and because $\langle n, m|f|n, m\rangle$ is positive definite (see Eq.(8.43)). This is not the case for single Pomeron exchange, where the e^{-f} factor is replaced by $1 - f$.

In the one-Pomeron exchange approximation, the formalism we have just described must be completely equivalent to the BFKL (leading $\ln s$) one, i.e. replacing the e^{-f} factor by $1 - f$ should lead to

$$S_1(\mathbf{r}_1, \mathbf{r}_2, \mathbf{b}, y) = 1 + F(r_1, r_2, b, y), \quad (8.46)$$

where $F(r_1, r_2, b, y)$ is defined in Eq.(8.17). It is enlightening to spend a little time outlining the proof of this equivalence.

We start by quoting the result (it is not hard to show):

$$e^{a_1} f[a^\dagger] e^{-a_1} = f[a^\dagger + 1], \tag{8.47}$$

where $f[a^\dagger]$ is some functional of the creation operator. Using Eq.(8.47), we can re-write Eq.(8.41) in the one-Pomeron exchange approximation as

$$\begin{aligned} S_1(r_1, r_2, b, y) &= 1 - \int d^2\mathbf{R} d^2\mathbf{R}' d^2\mathbf{c} d^2\mathbf{c}' f(\mathbf{R} - \mathbf{R}', \mathbf{c}, \mathbf{c}') \\ &\times \langle 0|a(\mathbf{R}', \mathbf{c}') e^{y'V_L[a^\dagger+1, a]} a^\dagger(\mathbf{b}_0, \mathbf{r}_1)|0\rangle \\ &\times \langle 0|d(\mathbf{R}, \mathbf{c}) e^{(y-y')V_R[d^\dagger+1, d]} d^\dagger(\mathbf{b} - \mathbf{b}_0, \mathbf{r}_2)|0\rangle. \end{aligned} \tag{8.48}$$

which, on comparison with Eq.(8.17), reveals that

$$\frac{n(r_1, c', y', R')}{2\pi c'^2} = \langle 0|a(\mathbf{R}', \mathbf{c}') e^{y'V_L[a^\dagger+1, a]} a^\dagger(\mathbf{b}_0, \mathbf{r}_1)|0\rangle. \tag{8.49}$$

We need to evaluate explicitly the right hand side of this expression and demonstrate its equivalence to the number density calculated using Eqs.(8.8) and (8.19).

Since the only terms in the exponent which generate a non-zero contribution to the number density are those which contain equal numbers of creation and annihilation operators we can make the replacement

$$V[1 + a^\dagger, a] \rightarrow a^\dagger K a. \tag{8.50}$$

Selecting terms in $V_1[1 + a^\dagger, a] + V_2[a^\dagger, a]$ (see Eqs.(8.32) and (8.33)) that contain one creation and one annihilation operator we find

$$a^\dagger K a \equiv \int d^2\mathbf{b} d^2\mathbf{x} d^2\mathbf{x}' d^2\mathbf{b}' a^\dagger(\mathbf{b} + \mathbf{b}', \mathbf{x}) K(\mathbf{b}', \mathbf{x}, \mathbf{x}') a(\mathbf{b}, \mathbf{x}') \tag{8.51}$$

and the evolution kernel is (using Eqs.(8.32) and (8.33))

$$\begin{aligned} K(\mathbf{b}', \mathbf{x}, \mathbf{x}') &= -\bar{\alpha}_s \ln \frac{x^2}{\rho^2} \delta^{(2)}(\mathbf{b}') \delta^{(2)}(\mathbf{x} - \mathbf{x}') \\ &+ \frac{\bar{\alpha}_s}{8\pi} \frac{\mathbf{x}'^2}{\mathbf{b}'^2 \mathbf{x}^2} \left[\delta^{(2)}(\mathbf{b}' + (\mathbf{x} + \mathbf{x}')/2) + \delta^{(2)}(\mathbf{b}' - (\mathbf{x} + \mathbf{x}')/2) \right]. \end{aligned} \tag{8.52}$$

The eigenfunctions of this operator are none other than the conformal eigenfunctions, i.e.

$$\begin{aligned} \int d^2\mathbf{b} \frac{d^2\mathbf{x}'}{\mathbf{x}'^4} K(\mathbf{b}' - \mathbf{b}, \mathbf{x}, \mathbf{x}') \tilde{\phi}_n^\nu(\mathbf{b} + \mathbf{x}'/2, \mathbf{b} - \mathbf{x}'/2, \mathbf{w}) \\ = \bar{\alpha}_s \chi_n(\nu) \frac{\tilde{\phi}_n^\nu(\mathbf{b}' + \mathbf{x}/2, \mathbf{b}' - \mathbf{x}/2, \mathbf{w})}{\mathbf{x}^4} \end{aligned} \tag{8.53}$$

and the eigenvalues are the eigenvalues of the BFKL kernel. To derive this important result, it is best to move to complex coordinates (i.e. $2d^2\mathbf{x} = dx d\bar{x}$) whereupon the integrand separates into a product of one-dimensional integrals over x and \bar{x} . After a change of variables the integrals can be rewritten in two-vector form, where they are seen to generate the eigenfunctions using the result that[†]

$$\int \frac{d^2\mathbf{z}}{2\pi} \frac{[2(\mathbf{z}^2)^{1/2+i\nu} - 1]}{\mathbf{z}^2(\mathbf{z} + \hat{\mathbf{n}})^2} = \chi_0(\nu), \tag{8.54}$$

where $\hat{\mathbf{n}}$ is an arbitrary unit vector. This result suggests that we should expand the dipole creation and annihilation operators in terms of these eigenfunctions, i.e.

$$a(\mathbf{b}, \mathbf{x}) = \sum_{n=-\infty}^{\infty} \int \frac{d\nu}{(2\pi)^2} 4(i\nu + n/2) a_{n\nu}(\mathbf{w}) \frac{d^2\mathbf{w}}{\mathbf{x}^4} \times \tilde{\phi}_n^\nu(\mathbf{b} + \mathbf{x}/2, \mathbf{b} - \mathbf{x}/2, \mathbf{w}), \tag{8.55}$$

and

$$a^\dagger(\mathbf{b}, \mathbf{x}) = \sum_{n=-\infty}^{\infty} \int \frac{d\nu}{(2\pi)^2} 4(-i\nu + n/2) a_{n\nu}^\dagger(\mathbf{w}) d^2\mathbf{w} \times \tilde{\phi}_n^{\nu*}(\mathbf{b} + \mathbf{x}/2, \mathbf{b} - \mathbf{x}/2, \mathbf{w}). \tag{8.56}$$

Using Eq.(4.50) the ‘conformal’ operators can be shown to satisfy the commutation relation

$$[a_{n\nu}(\mathbf{w}), a_{n'\nu'}^\dagger(\mathbf{w}')] = \delta_{nn'} \delta(\nu - \nu') \delta^{(2)}(\mathbf{w} - \mathbf{w}') \tag{8.57}$$

and, using the known properties of the eigenfunctions (Eqs.(8.4) and (8.5)), we can recast the evolution operator in the diagonal form

$$a^\dagger K a = \bar{\alpha}_s \sum_{n=-\infty}^{\infty} \int d\nu d^2\mathbf{w} \chi_n(\nu) a_{n\nu}^\dagger(\mathbf{w}) a_{n\nu}(\mathbf{w}). \tag{8.58}$$

Using Eqs.(8.55), (8.56), (8.57) and (8.58) in Eq.(8.49) allows us to show that (in the $n = 0$ case)

$$n(r_1, c, y, R) = 16 \int \frac{d\nu}{(2\pi)^3} \frac{d^2\mathbf{w}}{c^2} \nu^2 e^{\bar{\alpha}_s \chi_0(\nu)y} \tilde{\phi}_0^\nu(\mathbf{R} + \mathbf{c}/2, \mathbf{R} - \mathbf{c}/2, \mathbf{w}) \tilde{\phi}_0^{\nu*}(\mathbf{b}_0 + \mathbf{r}_1/2, \mathbf{b}_0 - \mathbf{r}_1/2, \mathbf{w}). \tag{8.59}$$

[†] This is appropriate for $n = 0$ but it is not much more difficult to prove the result for general n .

This is equivalent to the result that is obtained in a straightforward way after substituting Eq.(8.8) into Eq.(8.19).

Thus we have demonstrated the equivalence of the operator formalism to that of BFKL. Indeed, the dipole formalism does offer an alternative derivation of the BFKL equation (Mueller (1994, 1995), Mueller & Patel (1994), Chen & Mueller (1995), Nikolaev, Zakharov & Zoller (1994a,b), Nikolaev & Zakharov (1994)). However, more than merely reproducing the results obtained in Chapter 4 we have now established a framework in which we can investigate the multiple scattering corrections which motivated this alternative approach, i.e. we can go beyond the one-Pomeron exchange approximation.

8.2.2 Multiple scattering

Consider the total cross-section for the scattering of two primary dipoles of fixed (and equal) sizes R (this avoids us having to invoke specific onium wavefunctions and should demonstrate all the important features). It is natural to ask when the one Pomeron exchange approximation (BFKL) starts to break down. Formally the S -matrix for the elastic scattering can be written as a multiple scattering series; keeping only the first term corresponds to the BFKL calculation and has the S -matrix of Eq.(8.46). This will only be a good approximation provided $|F| \ll 1$. When $|F| \sim 1$ it becomes necessary to consider the remaining terms in the multiple scattering series. We shall discuss these terms shortly, but for now we have a simple condition for the validity of the BFKL calculation. We can evaluate $F(R, R, b, y)$ in the limit of $b^2 \gg R^2$ and for $a^2 y \gg \ln(b^2/R^2)$ (by the usual saddle point method). Our condition for the legitimate neglect of the multiple scattering corrections then becomes the explicit condition

$$-F(R, R, b, y) = 8\pi\alpha_s^2 \frac{R^2 \ln(b^2/R^2)}{b^2 (\pi a^2 y)^{3/2}} e^{\omega_0 y} \exp\left(-\frac{\ln^2(b^2/R^2)}{a^2 y}\right) \ll 1. \quad (8.60)$$

The total cross-section is formed using Eq.(8.20), i.e.

$$\sigma_{\text{tot}} = -2\pi \int db^2 F(R, R, b, y) = 8\pi R^2 \frac{\alpha_s^2 e^{\omega_0 y}}{(\pi a^2 y)^{1/2}}. \quad (8.61)$$

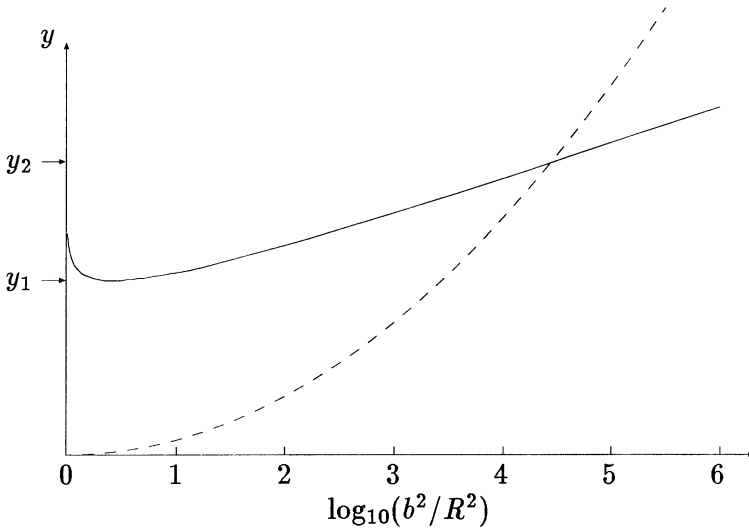


Fig. 8.3. Plot to delineate the region where the one-Pomeron exchange (BFKL) calculation (of the total cross-section) is valid from the region where multiple scattering is important.

The dominant contribution to this cross-section comes from the region of large b , in particular

$$b^2 \sim R^2 e^{\sqrt{a^2 y}} \quad (8.62)$$

and we have a self-consistent calculation (i.e. Eq.(8.60) is valid in the region which gives rise to the dominant contribution to the total cross-section). Note that the total cross-section is driven by the contribution from peripheral collisions (i.e. $b \gg R$). The inequality of Eq.(8.60) can be re-written as a bound on y at a given impact parameter, i.e. defining $y(b)$ to be the solution to $-F(R, R, b, y) = 1$ we find

$$\omega_0 y(b) \approx \ln \left(\frac{(\pi a^2 y(b))^{3/2}}{8\pi \alpha_s^2} \frac{b^2/R^2}{\ln(b^2/R^2)} \right) \quad (8.63)$$

and the condition for the validity of the one Pomeron exchange calculation of the amplitude at some impact parameter b is then that $y \ll y(b)$.

In Fig. 8.3, the solid line corresponds to the curve $y = y(b)$,

whilst the dashed line corresponds to $y = (1/a^2)\ln^2(b^2/R^2)$ (which, from Eq.(8.62), specifies the region which provides the dominant contribution to the total cross-section). We define y_1 to correspond to the minimum of the curve $y = y(b)$ and y_2 to be the rapidity where the two curves intersect. For $y < y_1$ the one Pomeron exchange approximation is appropriate over the whole range of impact parameter which contributes to the total cross-section and so we can trust the BFKL calculation in this region. For $y_1 < y < y_2$ multiple scattering corrections are significant for a wide range of impact parameter. However, the dominant contribution to the total cross-section still arises from the region of large impact parameter where the BFKL calculation is again valid. For $y > y_2$ multiple scattering corrections are now significant even in the region which contributes most to the total cross-section. Thus only for $y > y_2$ do we need to worry about the role of multiple scattering (unitarization) corrections to the total cross-section. Fig. 8.3 was produced with $\bar{\alpha}_s = 0.25$, in which case $y_1 \approx 15$, which is quite large and indicates that unitarity corrections to the total cross-section are important only at very high energies. The slow onset of the unitarity corrections is due essentially to the peripheral nature of the dominant contributions to the total rate, i.e. multiple scattering effects are most important for the more central collisions (where there is a large overlap between the left and right-moving dipole clusters).

A process which is more sensitive to the multiple scattering corrections will therefore be one which is dominated by more central collisions. The elastic-scattering cross-section is such a process. The integrated cross-section for elastic scattering is

$$\sigma_{\text{el}} = \pi \int db^2 |F(R, R, b, y)|^2 \quad (8.64)$$

and, since $|F| \sim 1/b^2$, it follows that the elastic cross-section is dominated by more central collisions than the total cross-section.

Having established when we expect the BFKL calculation to break down we turn now to a discussion of the specific nature of the multiple scattering corrections. Firstly we should establish the approximations that are inherent in deriving the particular form of the elastic scattering matrix of the preceding subsection, i.e. Eqs.(8.41) and (8.45). We know that the leading logarithmic

approximation of BFKL corresponds to the single scattering of one dipole in one onium with another dipole in the other onium, i.e. the S -matrix for elastic onium–onium scattering can be written

$$S = 1 + \alpha_s^2 \sum_{n=1}^{\infty} c_n(\bar{\alpha}_s y)^n. \quad (8.65)$$

We have distinguished between factors of α_s and factors of $\bar{\alpha}_s$. The latter factors are always accompanied by a logarithm of the energy since the leading logarithm approximation is also the leading $1/N$ approximation (N being the number of colours). The additional factor of α_s^2 arises due to the colour neutrality of the external onia. In the dipole picture, each onium evolves a dipole cloud by iterating the evolution operator, which is $\sim \bar{\alpha}_s y$. The interaction of the two dipoles is determined by $f \sim \alpha_s^2$. Clearly therefore, the n Pomeron exchange contribution is suppressed by the overall factor $\sim \alpha_s^{2n}$ – so it is sub-leading in both the $1/N$ and leading logarithm approximations. Why, therefore, do we keep these multiple scattering contributions whilst ignoring all the other possible higher order corrections?

The answer is simply stated: it is because of the very high numbers of dipoles which are generated in the evolution of the onia. Typical configurations contain very large numbers of dipoles, i.e. $\sim e^{\omega_0 y'}$ and $\sim e^{\omega_0(y-y')}$, so although the probability of an individual scattering is small ($\sim \alpha_s^2$) the number of ‘trials’ is very large (it is the product of the number of dipoles in each onium), i.e. $\sim e^{\omega_0 y}$. Thus we expect the multiple scattering corrections to be significant when $\alpha_s^2 e^{\omega_0 y} \sim 1$. The incoherent multiple scattering of the dipoles within the onia, i.e. the exponentiation of the basic dipole–dipole scattering amplitude (e^{-f}), amounts to the assumption that the dominant sub-leading effects are due solely to the large number of dipoles and that collective effects between the individual dipoles (which would spoil the exponentiation) are negligible. To make this plausible consider another sub-leading effect which should become important as the energy increases. This is the effect which we call **dipole saturation**. As the dipole evolution proceeds with the corresponding increase of the dipole number we might expect that dipoles within a single onium start to interact with other dipoles in the same onium. These effects are implemented via a modification of the onium wavefunction and are

$\sim \alpha_s^2 e^{\omega_0 y'}$ (i.e. the amplitude of any given dipole to interact with all the others is proportional to the number of dipoles). Clearly, if we choose to divide the rapidity interval equally between the two onia, i.e. $y' = y/2$, then the saturation effects enter at energies which are roughly the square of the energies where multiple scattering effects first become important. If we choose a highly asymmetric partitioning of the energy (e.g. $y' = 0$ or $y' = y$) then there is no justification for focusing only on the multiple scattering corrections, i.e. there will be large wavefunction saturation effects which alter the evolved onium state in such a way that the total amplitude is the same as that which would be obtained by including only multiple scattering effects but with $y' = y/2$. So, although the physics is clearly independent of y' the sensible choice is $y' = y/2$ since this maximally suppresses the saturation effects which we are unable to calculate. We expect all other sub-leading corrections to be truly sub-leading, i.e. not enhanced by large dipole multiplicity factors.

A word of caution ought to be issued at this stage. The above arguments rely heavily on the fact that the dominant features of the sub-leading corrections can be determined from knowledge of the average features of the dipole evolution. However, one can envisage scenarios where this is a dangerous line of reasoning. For example, consider a collision in the centre of mass (i.e. $y' = y/2$) at very large impact parameters, i.e. in the region where multiple scattering effects are small. One might also infer that saturation effects are therefore even smaller. However, this need not be the case. The dipole evolution could undergo a period of evolution where only small dipoles are produced. These large numbers of localized dipoles may then be subject to significant saturation corrections. In order to contribute to the scattering at large impact parameters at least one large dipole needs to be created (in at least one of the onia) and this may be done at the end of the dipole evolution. Thus the distribution of large dipoles can be affected by what happened earlier in the dipole evolution and hence be subject to large saturation corrections. However, for the typical configurations which provide the dominant contributions to, for example, the total cross-section we expect the more general arguments to hold (Mueller & Salam (1996)).

It is now time to investigate the actual size of the multiple scat-

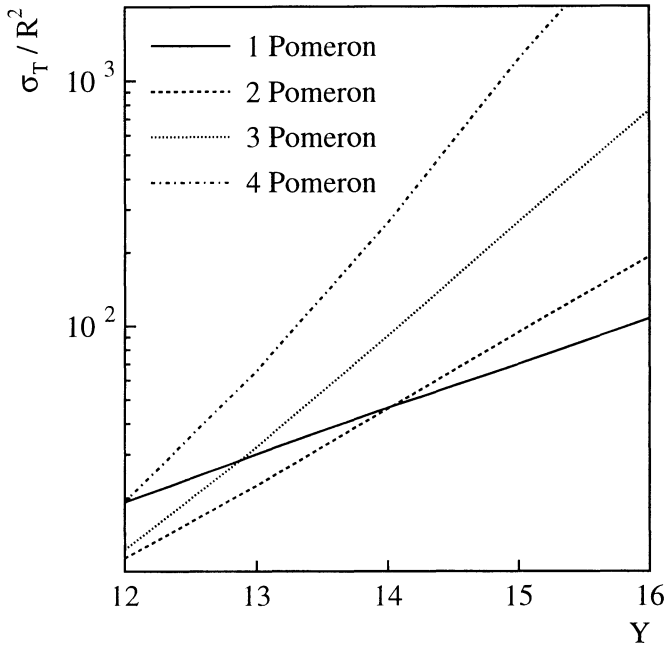


Fig. 8.4. The contributions to the total cross-section for the scattering of two primary dipoles of size R from successive terms in the multiple scattering series (see Salam (1996a)).

tering corrections. The natural course of action is to compute first the corrections to one Pomeron exchange which arise from the $f^2/2!$ term in the exponential series. Progress can be made with an analytic calculation. However, it is not necessary to go into the details here and so we refer to the work of Mueller (1995). The important feature is that the two Pomeron exchange contribution to the onium–onium total cross-section exceeds that for one Pomeron exchange for large enough y . This effect can be seen in Fig. 8.4, where the total cross-section for scattering two primary dipoles each of size R is shown (normalized by R^2). Moreover, and as Fig. 8.4 reveals, the contributions from even more Pomeron exchanges exceed the one Pomeron exchange contribution at

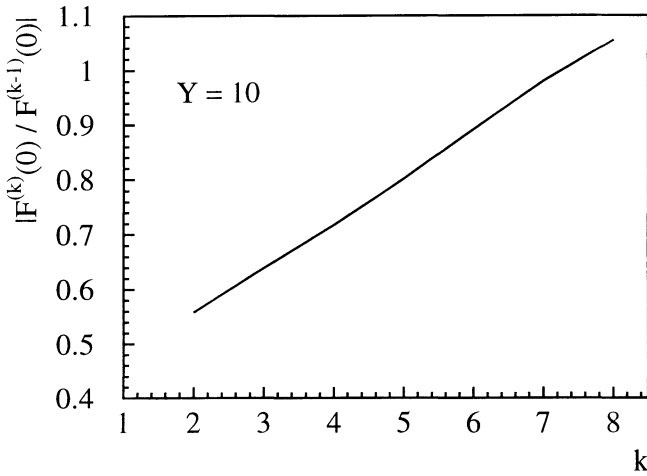


Fig. 8.5. The ratio of the elastic scattering amplitudes for k to $k-1$ Pomeron exchange. The amplitudes are computed at zero impact parameter (see Salam (1996a)).

successively lower energies. The curves are reproduced from the paper by Salam (1996a) using a Monte Carlo program (Salam (1996b)) and with $\alpha_s = 0.18$. Note that the nature of the dipole evolution is ideally suited to the construction of a Monte Carlo program which allows studies far more detailed than are possible analytically.

Some analytic progress has been made in establishing the essential features of the multiple scattering series. In particular, Mueller (1995) has introduced a toy model in which there are no transverse dimensions (i.e. the creation and annihilation operators have no arguments and satisfy $[a, a^\dagger] = 1$). This simplification allows complete analytic calculations to be performed. For large enough energies, the toy model suggests that the terms in the multiple scattering series are $\propto n!$ where n is the number of Pomeron exchanges. This behaviour also seems to hold to a good accuracy in the more realistic QCD case, as Fig. 8.5 shows. The graph shows the ratio of successive terms in the multiple scattering se-

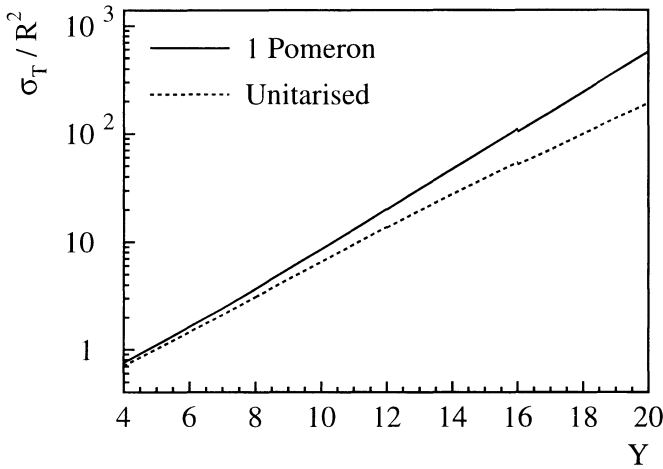


Fig. 8.6. The total cross-section for scattering primary dipoles of size R calculated with and without unitarization corrections (see Salam (1996a)).

ries (for elastic scattering of two primary dipoles at zero impact parameter and fixed energy) and the linearity confirms the factorial behaviour of the terms in the series. This explains the origin of the apparent divergence of the multiple scattering series which is seen in Fig. 8.4. Thus it seems necessary to sum up the whole series before making any predictions. The (summed) large order behaviour of this series cancels out for small enough rapidities even though the individual terms each yield very large contributions. This means that the one Pomeron exchange contribution is good provided the S -matrix is close to unity (as discussed earlier) but as soon as the double Pomeron exchange contribution starts to become important so, too, do all other Pomeron exchanges. The well behaved nature of the fully summed multiple scattering series and the relative smallness of the multiple scattering effects for $y \lesssim 10$ (which is roughly in line with our expectations from the start of this subsection) can be seen in Fig. 8.6, where the total cross-section is shown as a function of rapidity.

To conclude, we have shown how to unitarize the scattering amplitude. Unitarization, via multiple interactions, occurs in the perturbative domain (for small enough primary dipoles). However, non-perturbative physics is ultimately required in order to ensure that the total cross-section satisfies the Froissart–Martin bound (any calculation which assumes massless exchanges, as we do, need not obey that bound). We argued that multiple scattering is the largest unitarization effect. Also, for large enough energies, we argued that the effects of wavefunction saturation can no longer be ignored. Ultimately, the total cross-section becomes dominated by non-perturbative effects. We should also like to remind the reader that we have been working with primary dipoles which are small in size (e.g. dipoles arising from heavy onia). If the colliding particles are light hadrons then the small size configurations are relatively rare fluctuations and lead to small corrections compared with the predominant contribution from non-perturbative physics.

8.3 Summary

- High energy scattering in QCD can be viewed as the scattering of dipole clusters which are generated by the incoherent branching of one dipole into two dipoles. We demonstrated the equivalence of this approach to the one of BFKL developed earlier. The dipole picture provides a very convenient description of high energy scattering in terms of the locations of the dipoles in impact parameter space.
- In QCD the leading logarithm approximation to high energy scattering leads to a power-like growth of total cross-sections, i.e. $\sim s^{\omega_0}$. This growth leads to the violation of unitarity at high enough energies. We quantify when this violation is expected to occur.
- The dipole language of high energy scattering was derived within an operator formalism. This formalism is also suitable for the calculation of the important corrections (to the leading logarithm calculation) which ensure the preservation of unitarity. These corrections arise due to the large number of dipoles within the colliding particles leading to a significant probability that more than one pair of dipoles will interact per onium–onium collision.

8.4 Appendix A

In this appendix we outline the derivation of Eq.(8.7). Our starting point is the relation,

$$\begin{aligned} \frac{F(s, \mathbf{k}_1, \mathbf{k}_2, \mathbf{q})}{\mathbf{k}_2^2(\mathbf{k}_1 - \mathbf{q})^2} &= \frac{1}{(2\pi)^2} \int d^2\mathbf{b}_{11'} d^2\mathbf{b}_{22'} d^2(\mathbf{b}'_1 - \mathbf{b}'_2) \\ &\times e^{-i(\mathbf{k}_1 \cdot \mathbf{b}_{11'} - \mathbf{k}_2 \cdot \mathbf{b}_{22'} + \mathbf{q} \cdot (\mathbf{b}'_1 - \mathbf{b}'_2))} \\ &\times (\partial_{\mathbf{b}'_1}^2 \partial_{\mathbf{b}'_2}^2)^{-1} \hat{f}(y, \mathbf{b}_1, \mathbf{b}'_1, \mathbf{b}_2, \mathbf{b}'_2), \end{aligned} \tag{A.8.1}$$

which is just the inverse transform of Eq.(4.46).

We now make use of the convolution formula, Eq.(8.6), to replace \hat{f} by a convolution of two \hat{f} factors; after a simple manipulation we find (again using Eq.(4.51) with $n = 0$)

$$\begin{aligned} \frac{F(s, \mathbf{k}_1, \mathbf{k}_2, \mathbf{q})}{\mathbf{k}_2^2(\mathbf{k}_1 - \mathbf{q})^2} &= \frac{1}{(2\pi)^2} \int d^2\mathbf{b}_{11'} d^2\mathbf{b}_{22'} d^2(\mathbf{b}'_1 - \mathbf{b}'_2) \\ &\times \frac{1}{\pi^8} \int \frac{d^2\mathbf{b}_x d^2\mathbf{b}'_x}{\mathbf{b}_{\mathbf{x}\mathbf{x}'^4}} d^2\mathbf{c} d^2\mathbf{c}' e^{-i(\dots)} \\ &\times \frac{1}{16} \int d\nu \frac{\nu^2}{(\nu^2 + 1/4)^2} \int d\mu \mu^2 e^{\alpha_s(\chi_0(\nu)y' + \chi_0(\mu)(y-y'))} \\ &\times \tilde{\phi}_0^\nu(\mathbf{b}_1, \mathbf{b}'_1, \mathbf{c}) \tilde{\phi}_0^{\nu*}(\mathbf{b}_x, \mathbf{b}'_x, \mathbf{c}) \tilde{\phi}_0^\mu(\mathbf{b}_x, \mathbf{b}'_x, \mathbf{c}') \tilde{\phi}_0^{\mu*}(\mathbf{b}_2, \mathbf{b}'_2, \mathbf{c}'), \end{aligned} \tag{A.8.2}$$

where $\mathbf{b}_{\mathbf{x}\mathbf{x}'} = \mathbf{b}_x - \mathbf{b}_{x'}$.

Now we insert the delta function operator:

$$\begin{aligned} &\delta^2(\mathbf{b}_x - \mathbf{b}_y) \delta^2(\mathbf{b}'_x - \mathbf{b}'_y) + \delta^2(\mathbf{b}_x - \mathbf{b}'_y) \delta^2(\mathbf{b}'_x - \mathbf{b}_y) \\ &= \frac{1}{2(2\pi)^4} \partial_{\mathbf{b}_y}^2 \partial_{\mathbf{b}'_y}^2 \int \frac{d^2\mathbf{l}_1}{\mathbf{l}_1^2} \frac{d^2\mathbf{l}_2}{\mathbf{l}_2^2} \\ &\times \left[e^{i\mathbf{l}_1 \cdot (\mathbf{b}_x - \mathbf{b}_y)} - e^{i\mathbf{l}_1 \cdot (\mathbf{b}_x - \mathbf{b}'_y)} - e^{i\mathbf{l}_1 \cdot (\mathbf{b}'_x - \mathbf{b}_y)} + e^{i\mathbf{l}_1 \cdot (\mathbf{b}'_x - \mathbf{b}'_y)} \right] \\ &\times \left[e^{i\mathbf{l}_2 \cdot (\mathbf{b}_x - \mathbf{b}_y)} - e^{i\mathbf{l}_2 \cdot (\mathbf{b}_x - \mathbf{b}'_y)} - e^{i\mathbf{l}_2 \cdot (\mathbf{b}'_x - \mathbf{b}_y)} + e^{i\mathbf{l}_2 \cdot (\mathbf{b}'_x - \mathbf{b}'_y)} \right]. \end{aligned} \tag{A.8.3}$$

Since the eigenfunctions, $\tilde{\phi}_0^\mu(\mathbf{b}_1, \mathbf{b}_2, \mathbf{c})$, are symmetric under the interchange of the first two arguments (i.e. $\mathbf{b}_1 \leftrightarrow \mathbf{b}_2$) we can insert the delta functions of Eq.(A.8.3). Note that the \mathbf{l}_i integrals are finite *before* the action of the Laplacian operators – we utilized the symmetry property of the eigenfunctions under interchange of the arguments to ensure just this property. As a result, we

can perform an integration by parts to reverse the action of the Laplacian operators such that they act upon the eigenfunctions rather than the \mathbf{l} integrand. Hence,

$$\begin{aligned} \frac{F(s, \mathbf{k}_1, \mathbf{k}_2, \mathbf{q})}{\mathbf{k}_2^2(\mathbf{k}_1 - \mathbf{q})^2} &= \frac{1}{4(2\pi)^6} \int d^2\mathbf{b}_{11'} d^2\mathbf{b}_{22'} d^2(\mathbf{b}'_1 - \mathbf{b}'_2) e^{-i(\dots)} \\ &\times \int \frac{d^2\mathbf{b}_x d^2\mathbf{b}'_x}{\mathbf{b}_{xx'}^4} \frac{d^2\mathbf{b}_y d^2\mathbf{b}'_y}{\mathbf{b}_{yy'}^4} d^2\mathbf{c} d^2\mathbf{c}' \frac{d^2\mathbf{l}_1}{\mathbf{l}_1^2} \frac{d^2\mathbf{l}_2}{\mathbf{l}_2^2} [\dots][\dots] \\ &\times \frac{1}{\pi^8} \int d\nu \nu^2 \int d\mu \mu^2 e^{\tilde{\alpha}_s(\chi_0(\nu)y' + \chi_0(\mu)(y-y'))} \\ &\times \tilde{\phi}'_0(\mathbf{b}_1, \mathbf{b}'_1, \mathbf{c}) \tilde{\phi}^{\nu*}(\mathbf{b}_y, \mathbf{b}'_y, \mathbf{c}) \tilde{\phi}^\mu(\mathbf{b}_x, \mathbf{b}'_x, \mathbf{c}') \tilde{\phi}^{\mu*}(\mathbf{b}_2, \mathbf{b}'_2, \mathbf{c}'). \end{aligned} \tag{A.8.4}$$

Making the standard change of variables

$$\mathbf{R}_x = \frac{1}{2}(\mathbf{b}_x + \mathbf{b}_{x'}) - \mathbf{c}',$$

and similarly for the other co-ordinates, allows the volume elements to be re-written, i.e.

$$\begin{aligned} d^2(\mathbf{b}'_1 - \mathbf{b}'_2) d^2\mathbf{c} d^2\mathbf{c}' &\rightarrow d^2(\mathbf{c} - \mathbf{c}') d^2\mathbf{R}_1 d^2\mathbf{R}_2 \\ d^2\mathbf{b}_x d^2\mathbf{b}'_x &\rightarrow d^2\mathbf{R}_x d^2\mathbf{b}_{xx'}, \quad \text{etc.} \end{aligned} \tag{A.8.5}$$

The independent variables are now $\mathbf{b}_{11'}$, $\mathbf{b}_{22'}$, \mathbf{R}_1 , \mathbf{R}_2 , $\mathbf{b}_{xx'}$, $\mathbf{b}_{yy'}$, \mathbf{R}_x , \mathbf{R}_y and $\mathbf{c} - \mathbf{c}'$. The only dependence upon $\mathbf{c} - \mathbf{c}'$ is in the exponential terms. Hence we can collect them together and integrate over $\mathbf{c} - \mathbf{c}'$ which gives the delta function factor $(2\pi)^2 \delta^2(\mathbf{q} - \mathbf{l}_1 - \mathbf{l}_2)$.

The remaining integrals, combined with the definitions specified by Eqs.(8.8) and (8.9), lead directly to the desired result, i.e. Eq.(8.7).

8.5 Appendix B

In this appendix we derive Eq.(8.27) for the probability of emission of a gluon from a dipole.

Consider a colour singlet dipole with momentum p_1 moving along the positive z -axis. It is convenient to define a momentum p_2 with the same energy component moving along the negative z -axis, such that $2p_1 \cdot p_2 = s$.

Let $\psi(\rho_0, \mathbf{r})$ be the amplitude for this dipole to consist of a quark-antiquark pair in which the quark carries a fraction ρ_0

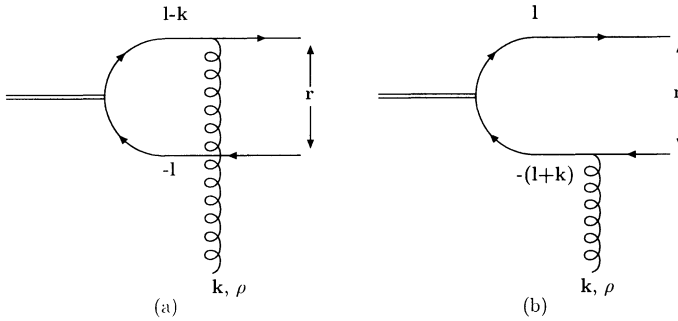


Fig. 8.7. Graphs for the emission of a gluon from a dipole.

of the longitudinal momentum of the dipole and is separated from the antiquark, in impact parameter space, by \mathbf{r} . We may write this in terms of an amplitude in transverse momentum space as

$$\psi(\rho_0, \mathbf{r}) = \frac{1}{(2\pi)^2} \int d^2\mathbf{l} e^{i\mathbf{l}\cdot\mathbf{r}} \tilde{\psi}(\rho_0, \mathbf{l}), \tag{B.8.1}$$

where $\tilde{\psi}(\rho_0, \mathbf{l})$ is the amplitude for the quark to have transverse momentum \mathbf{l} and the antiquark to have transverse momentum $-\mathbf{l}$.

Now consider a gluon with transverse momentum \mathbf{k} and fraction of longitudinal momentum ρ emitted from this dipole, as shown in Fig. 8.7. We assume that $\rho \ll \rho_0, (1 - \rho_0)$. This is the strong ordering required for the leading logarithm approximation. This gluon will later couple to a further gluon so it is really off-shell. However, since any gluon to which it couples has a fraction of longitudinal momentum which is small compared with that of the parent gluon and transverse momentum which is small compared with the longitudinal momentum of the parent, it is a valid approximation to consider the emitted gluon to be on shell (and hence transversely polarized). The rapidity of the emitted gluon is given by

$$y = \frac{1}{2} \ln (s\rho^2/\mathbf{k}^2). \tag{B.8.2}$$

We may write the momenta of the quark and antiquark as

$$l_1^\mu = \rho_0 p_1^\mu + \frac{\mathbf{l}^2}{s\rho_0} p_2^\mu + l_{\perp}^\mu, \tag{B.8.3}$$

$$l_2^\mu = (1 - \rho_0)p_1^\mu + \frac{\mathbf{l}^2}{s(1 - \rho_0)}p_2^\mu - l_{\perp}^\mu, \quad (\text{B.8.4})$$

and the momentum of the emitted gluon as

$$k^\mu = \rho p_1^\mu + \frac{\mathbf{k}^2}{s\rho}p_2^\mu + k_{\perp}^\mu. \quad (\text{B.8.5})$$

Furthermore we can exploit gauge invariance to demand that the polarization vector, e^μ , of the emitted gluon has no component proportional to p_1^μ and, using the fact that the gluon is transverse ($e \cdot k = 0$), we have

$$e^\mu = \frac{2\mathbf{e} \cdot \mathbf{k}}{s\rho}p_2^\mu + e_{\perp}^\mu. \quad (\text{B.8.6})$$

Now the amplitude for emission from the quark (Fig. 8.7(a)) is

$$- ig\tau^a \frac{2l_1 \cdot e}{2l_1 \cdot k} \tilde{\psi}(\rho_0, \mathbf{l} - \mathbf{k}/2), \quad (\text{B.8.7})$$

where the factor $\tilde{\psi}(\rho_0, \mathbf{l} - \mathbf{k}/2)$ indicates that the quark–antiquark pair produced by the dipole are separated by $2\mathbf{l} - \mathbf{k}$ in transverse momentum space. τ^a is the colour generator in the fundamental representation. We have used the eikonal approximation as the emitted gluon is soft relative to the parent quark.

For $\rho \ll \rho_0$, we may use Eqs.(B.8.3), (B.8.5) and (B.8.6) to write

$$2l_1 \cdot e = \frac{2\rho_0\mathbf{e} \cdot \mathbf{k}}{\rho}$$

$$2l_1 \cdot k = \frac{\rho_0\mathbf{k}^2}{\rho}$$

(we have kept only the terms proportional to $1/\rho$), so that the contribution from this graph becomes

$$- 2ig\tau^a \frac{\mathbf{e} \cdot \mathbf{k}}{\mathbf{k}^2} \tilde{\psi}(\rho_0, \mathbf{l} - \mathbf{k}/2). \quad (\text{B.8.8})$$

Likewise the contribution from emission off the antiquark (Fig. 8.7(b)) is

$$2ig\tau^a \frac{\mathbf{e} \cdot \mathbf{k}}{\mathbf{k}^2} \tilde{\psi}(\rho_0, \mathbf{l} + \mathbf{k}/2). \quad (\text{B.8.9})$$

Returning to impact parameter space the total amplitude for the emission of the gluon off a dipole with transverse size \mathbf{r} is

$$\begin{aligned}
 & -2ig\tau^a \frac{\mathbf{e} \cdot \mathbf{k}}{\mathbf{k}^2} \frac{1}{(2\pi)^2} \int d^2\mathbf{l} e^{i\mathbf{l} \cdot \mathbf{r}} \left(\tilde{\psi}(\rho_0, \mathbf{l} - \frac{\mathbf{k}}{2}) - \tilde{\psi}(\rho_0, \mathbf{l} + \frac{\mathbf{k}}{2}) \right) \\
 &= -2ig\tau^a \frac{\mathbf{e} \cdot \mathbf{k}}{\mathbf{k}^2} e^{-i\frac{1}{2}\mathbf{k} \cdot \mathbf{r}} \frac{1}{(2\pi)^2} \int d^2\mathbf{l} e^{i\mathbf{l} \cdot \mathbf{r}} \tilde{\psi}(\rho_0, \mathbf{l}) (1 - e^{i\mathbf{k} \cdot \mathbf{r}}) \\
 &= -2ig\tau^a \frac{\mathbf{e} \cdot \mathbf{k}}{\mathbf{k}^2} e^{-i\frac{1}{2}\mathbf{k} \cdot \mathbf{r}} \psi(\rho_0, \mathbf{r}) (1 - e^{i\mathbf{k} \cdot \mathbf{r}}). \tag{B.8.10}
 \end{aligned}$$

Taking the square modulus of this and summing over emitted gluon polarizations and colours gives us

$$4g^2 \frac{N^2 - 1}{N} \frac{|\psi(\rho_0, \mathbf{r})|^2}{\mathbf{k}^2} (1 - e^{i\mathbf{k} \cdot \mathbf{r}}) \tag{B.8.11}$$

(where we understand that we must take the real part of the exponential). The factor of $(N^2 - 1)/2N$ comes from the square of the colour generator summed over all possible colours for the emitted gluon. In the large N limit we may replace this by $N/2$ (this allows us to generalize our result without modification, so that it describes gluon emission off any colour dipole, i.e. not just a $q-\bar{q}$ pair). It is worth noting here that this expression is proportional to the impact factor for the coupling of a (zero momentum transfer) Pomeron to the parent dipole. The formalism is easily extended to non-zero momentum transfer.[†]

The element of phase space is given by

$$\frac{1}{2(2\pi)^3} d^2\mathbf{k} \frac{d\rho}{\rho}.$$

We may use Eq.(B.8.2) to express this in terms of rapidity and obtain

$$\frac{1}{2(2\pi)^3} d^2\mathbf{k} dy.$$

Thus the probability of emitting a gluon into a rapidity interval dy and transverse momentum interval $d^2\mathbf{k}$ is

[†] For non-zero momentum transfer, we need to multiply Eq.(B.8.10) by the conjugate of the amplitude which is obtained by replacing $\mathbf{k} \rightarrow \mathbf{k} - \mathbf{q}$ in Eq.(B.8.10). This adds extra exponential factors in the final result as well a factor of $(\mathbf{e} \cdot \mathbf{k})(\mathbf{e} \cdot (\mathbf{k} - \mathbf{q}))$. The latter factor poses no problem, on using Eq.(8.29), whilst the former (on transforming to impact parameter space) leads to delta functions which fix the locations of the dipoles (i.e. the arguments of the creation and annihilation operators of Eq.(8.32)).

$$\frac{\bar{\alpha}_s}{\pi} \frac{d^2\mathbf{k}}{\mathbf{k}^2} dy (1 - e^{i\mathbf{k}\cdot\mathbf{r}}) |\psi(\rho_0, \mathbf{r})|^2. \quad (\text{B.8.12})$$

The factor $|\psi(\rho_0, \mathbf{r})|^2$ is just the probability of finding the dipole in the first place. Therefore the probability for emission of a gluon from a dipole is given by Eq.(8.27).